International Journal of Nanomedicine

Dovepress
open access to scientific and medical research

Open Access Full Text Article

ORIGINAL RESEARCH

Synergy of Polydopamine Nanovaccine and Endostar Alginate Hydrogel for Improving Antitumor Immune Responses Against Colon Tumor

Ying Yang[1], Ning Wang[2], XinXin Tian[1], XiaoLi Wang[1], Jing Yang[1], XiGang Leng[1], HaiLing Zhang[1]

[1]Institute of Biomedical Engineering, Chinese Academy of Medical Sciences & Peking Union Medical College, Tianjin Key Laboratory of Biomaterials, Tianjin, People's Republic of China; [2]Key Laboratory of Colloid and Interface Chemistry of the Ministry of Education, School of Chemistry and Chemical Engineering, Shandong University, Jinan, People's Republic of China

Correspondence: HaiLing Zhang, Institute of Biomedical Engineering, Chinese Academy of Medical Sciences & Peking Union Medical College, Tianjin Key Laboratory of Biomaterials, Tianjin, People's Republic of China, Tel +86 22 8789 1191, Fax +86 22 8789 0153, Email zhanghl@bme.pumc.edu.cn

Background: Tumor immunotherapy, a novel type of therapeutic treatment, has a wide range of applications with potentially prolonged benefits. However, current immunotherapy has a low overall response rate in treating a variety of tumors. Combination of immunotherapy with other therapies can improve the therapeutic response rates. The purpose of this work was to explore the potential of anti-angiogenic treatment in combination with tumor cell lysate loaded polydopamine nanoparticle vaccine as a therapeutic strategy for colon tumor.

Methods: We grafted tumor cell lysate onto polydopamine nanoparticles as nano-vaccine (TCLN) and fabricated alginate hydrogel loaded with Endostar (EH), then detected characteristics of EH and TCLN. We also estimated the cytotoxicity of EH/TCLN in vitro. In the tumor-bearing mouse model, we evaluated the antitumor effect of EH/TCLN treatment, and developed the animal survival study. After performing the EH/TCLN treatment, we also analyzed T cells and DCs using flow cytometry, and determined T cell responses and tumor microenvironmental cytokines. At last, we assessed the effect of the EH/TCLN treatment on anti-angiogenesis further.

Results: When applied in combination with TCLN in MC-38 tumor-bearing mice, EH/TCLN significantly suppressed tumor growth with more than half of the mice showing tumor regression. In addition, EH/TCLN treatment resulted in noticeable changes in the tumor microenvironment. As compared with the control group, EH/TCLN treatment led to significantly reduced tumor angiogenesis and expression of tumor microenvironment-related cytokines (TMCs), increased proportion of $CD8^+$ T cells in the spleen, lymph node and tumor, elevated activity of cytotoxic T lymphocytes (CTLs) and tumor cell apoptosis.

Conclusion: The present study demonstrated that the EH/TCLN treatment effectively created a favorable immune microenvironment for the induction of antitumor immunity and improved antitumor immune responses.

Keywords: alginate, polydopamine, Endostar, colon tumor, angiogenesis, immunotherapy

Introduction

Tumor immunotherapy has several advantages compared to other tumor treatments, including low toxicity, a wide range of applications, and probable prolonged benefits.[1] However, current immunotherapy has a relatively low overall response rate (ORR).[2] In a 2017 study on 15 types of tumors such as glioblastoma, head and neck tumor, breast tumor and colorectal tumor, less than 15% of the patients had clinical response to the immunotherapy.[3] The dendritic cell (DC) vaccine loaded with tumor antigens is an active approach for immunization. The nano-DC vaccine prepared using biomaterials, has achieved excellent results in preclinical experiments, including enhancing DC antigen presentation capability, triggering robust antitumor immune response, and inhibiting primary or metastatic tumor growth.[4–6] Notably, the immunization effect of nano-vaccine could be affected by multiple factors such as the choice of tumor antigens, strong tumor variability, and tumor immunosuppressive microenvironment.[7] Until recently, its results of clinical trials remain less than satisfactory, suggesting that mono-immunotherapy cannot persistently elicit an effective antitumor immunity in vivo. Combination of immunotherapy with other therapies may improve the therapeutic

Received: 3 May 2022
Accepted: 13 September 2022
Published: 12 October 2022

Graphical Abstract

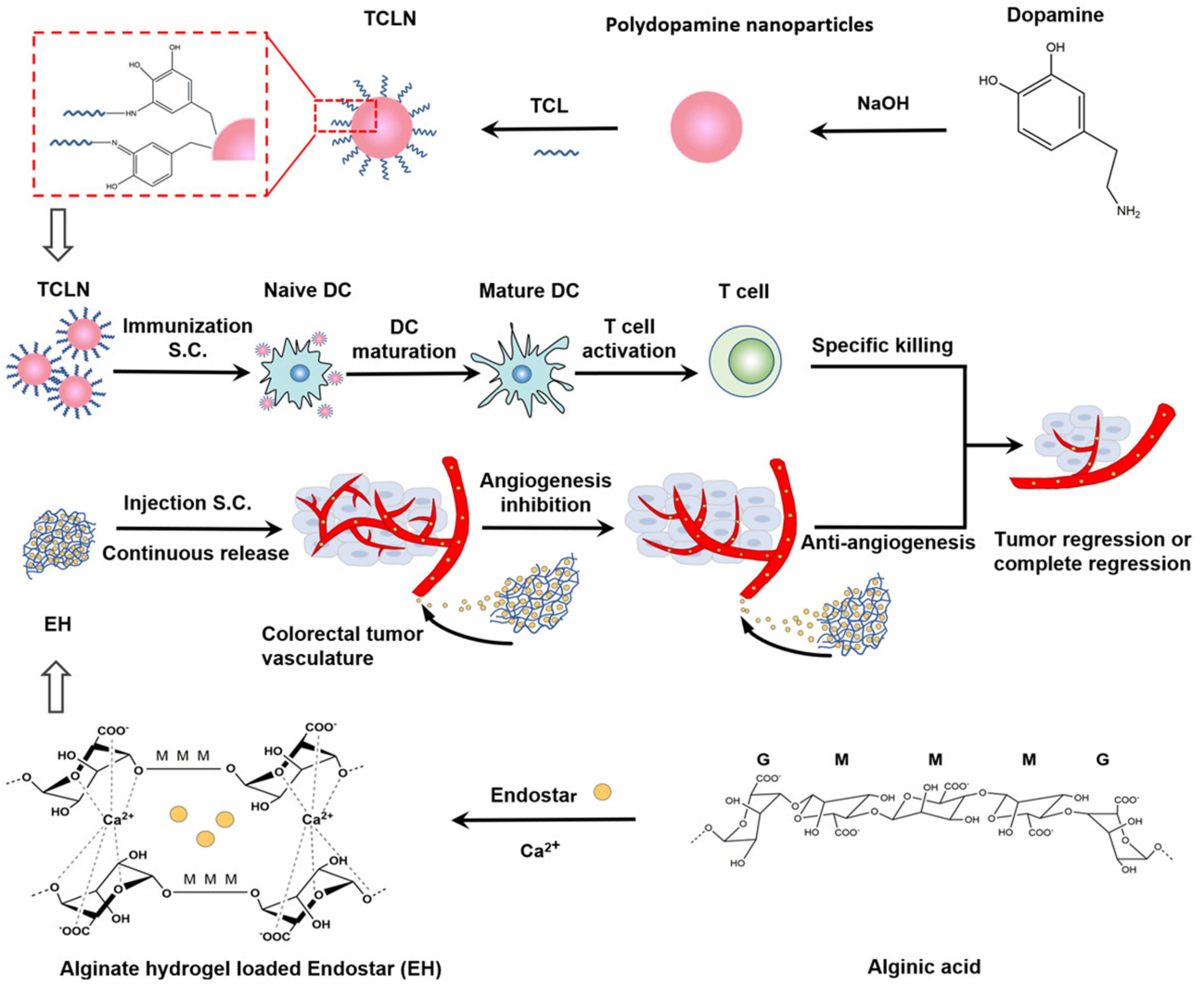

response rates and could therefore be a key driving force for exciting total potential capability of nano-DC vaccines in tumor immunotherapy.

Growing research have shown that there are multiple mechanisms involved in the process of anti-angiogenic therapy, including immune regulation mechanisms,[8] and that the anti-angiogenic therapy can weaken various immune-suppressing networks induced by tumors.[9] Endostatin is an endogenous anti-angiogenic polypeptide targeting endothelial cells, which has been proven as an effective antitumor drug in more than 65 different types of tumors.[10] Endostar is a commercially available recombinant human endostatin with high activity and low cost.[11] Recent report[12] and our previous research have shown that Endostar was able to downregulate the expression of TMCs including IL-6, IL-10, IL-17 and TGF-β, upregulate the expression of antitumor immune factor IFN-γ, promote migration of mature DCs and $CD8^+$ T cells into tumor microenvironment. Therefore, it was feasible to use Endostar to effectively relieve the immunosuppressive tumor microenvironment[10] and potentially enhance antitumor immunity.[13]

Combining tumor nano-vaccines with anti-angiogenesis may be a promising strategy that may effectively combating tumors. Here, we postulate that application of alginic hydrogel loaded with Endostar in combination with TCLN might achieve synergistic

antitumor effect in colon tumor. The TCLN nano-vaccine has an ability to strongly trigger the antitumor immune response by controlling the size of polydopamine nanoparticles (PDA).[14] On the other hand, alginate is an acidic, colloid polysaccharide that has the merits of excellent biocompatibility, nontoxicity, non-immunogenicity, and good biodegradability.[15] Many studies have reported the potential use of alginate-based platforms as effective vehicles for drug delivery,[16] and alginate hydrogels are considered to have easy drug loading ability and high loading capacity for many therapeutic agents under mild reaction conditions.[17] In this study, the alginic hydrogel has been used to sustain the release anti-angiogenic Endostar, that could not only reduce toxicity in the cardiovascular system,[18] but also maintain an effective systemic concentration, leading to significant inhibition of tumor growth and immune regulation of tumor microenvironment. The current study aimed at exploring the effect of Endostar hydrogel in combination with TCLN on tumor growth and survival rate of colon tumor in mice, and assessing the influence of combination therapy on the intratumoral microenvironment and immune response in vivo. Moreover, the possible link between active immunotherapy and anti-angiogenic therapy was also investigated.

Materials and Methods

Cell Lines and Animals

Mouse colon carcinoma cell line MC-38 and murine fibroblast cell line NIH3T3 were purchased from BeNa Culture Collection (China). Pathogen-free Sprague–Dawley (SD) rats and C57BL/6 mice were purchased from Beijing Sibeifu Experimental Animal Center (China). The overall project protocols had been reviewed and approved by the Animal Ethical and Welfare Committee of Institute of Radiation Medicine, Chinese Academy of Medical Sciences (Approval No. IRM-DWLL-2019128). All experiments with mice were performed following the established guidelines of the National Standards of People's Republic of China (GB/T 35892–2018).

Materials

Alginate sodium (160 mPa·s viscosity) with low G/M ratio was purchased from Qingdao Crystal Salt Bioscience and Technology Corporation (China). The G/M ratio of the alginate sodium was 1:3, as determined by circular dichroism (CD) spectrometer.[19] Endostar was bought from Shandong Xiansheng Maidejin Biological Pharmaceutical Co., Ltd (China). Dopamine hydrochloride was purchased from Yuancheng Technology Development Co., Ltd. (China). Mouse VEGF, matrix metalloproteinase-9 (MMP-9), IL-8 and IL-17 ELISA kits were obtained from Shanghai Enzyme-Linked Biotechnology Co., Ltd. (China). Mouse IFN-γ, TNF-α, IL-4, IL-6, IL-10 and IL-12 ELISA kits, and CD11c-PerCP-Cyanine5.5, MHCI-APC and CD86-PE were the products of eBioscience (USA). Mouse monoclonal antibodies MHCII-FITC, CD3-PerCP/Cyanine5.5, CD8-APC and CD4-FITC were purchased from BioLegend (USA). MTT Cell Proliferation and Cytotoxicity Assay Kit, penicillin, streptomycin and goat serum were purchased from Beyotime (China). In situ Cell Death Detection Kit (POD), Drabkin's reagent, and hemoglobin standard were obtained from Sigma-Aldrich, Inc. (USA). RPMI-1640 medium and heat-inactivated FBS were purchased from Biological Industries (Israel).

Preparation of Alginate Hydrogel Loaded with Endostar (EH)

EH was prepared as previously reported with minor modifications.[20] In brief, different concentrations of sodium alginate solution were prepared with 4 mL of deionized water, and then mixed with 2 mL of Endostar solution (15 mg/mL). EDTA-$CaCl_2$ solution (100 mM) was prepared with pH adjusted to 3.5 using HCl. Finally, 1 mL of EDTA-Ca solution was added dropwise in the alginate solutions to form the desired hydrogel with continually stirring for 0.5 h. The EH was obtained by dialyzing against deionized water for 12 h and stored at 4 °C for further use. Morphology of EH was observed with a scanning electron microscope (SEM, Zeiss Gemini 300, Germany). The Ca^{2+} concentration of EH was determined by measuring the content of calcium element using an Inductively Coupled Plasma Emission Spectrometer (ICP-OES, SPECTROBLUE, Germany).

Encapsulation Efficiency Assessment

Two milliliters of EH was dissolved in 5 mL of PBS at RT for 1 h with continuously stirring, and then the supernatant was collected after centrifugation (10,000 g, 10 min). The drug concentration in the supernatant was estimated using enzyme-linked immunosorbent assay (ELISA). Each sample was assayed in triplicates. The encapsulation efficiency (EE)

was expressed by relating the actual entrapped Endostar to the theoretical Endostar amount. The Endostar content (EC) was described by the entrapped Endostar as a weight percentage of EH.

EH Release Study

In vitro Release

The release rate of Endostar from EH was evaluated as described previously.[21] Two milliliters of EH was mixed with 1 mL of PBS, and shaken with a rotary shaker at 200 rpm and 37°C. At the predetermined intervals, 1 mL of supernatant was collected and equal volume of fresh buffer was added. The amount of Endostar in the supernatant was determined by ELISA (Abcam, UK) according to the manufacturer's instructions. The cumulative release of Endostar was given as a function of time.

In vivo Release

The in vivo release of Endostar from EH was evaluated with SD rats. Briefly, EH was subcutaneously (s.c.) administrated to the right flank of rats at a dose of 147 mg/kg EH containing 20 mg of Endostar. Blood samples were collected at different time intervals for the duration of 26 days. Endostar concentrations in the blood samples were determined by ELISA according to the manufacturer's instructions. Data were presented as mean ± standard deviation.

Preparation of TCLN

TCLN was prepared as reported in our previous publication.[14] Two milligrams per milliliter of dopamine solution was mixed with 3.36 mg of 1 M NaOH solution at 50°C under vigorous stirring for 3 hours, and then PDA were collected by centrifugation (19,000 g, 10 min) and resuspended in 2 mL of deionized water. Then, 0.5 mL of PDA suspension and 5 mL of TCL solution (0.6 mg/mL) were mixed with stirring for 5 hours, and the resulted TCLN was harvested by centrifugation (19,000 g, 10 min). The TCL loading capacity was 491±16.3 μg/mg determined by measuring the content of sulfur element using the ICP-OES. The characterization of PDA such as the average particle size and zeta potential were measured using Nano-ZS 90 (Malvern Instrument, UK). Cytotoxicity assays of the AH, AH/PDA, and EH/TCLN groups were reported in Supplementary Method.

Antitumor Effect of EH/TCLN in the Tumor-Bearing Mice

Six-to-eight-week-old female C57BL/6 mice were injected s.c. with 1×10^6 MC38 cells in 0.1 mL PBS at the right flank as primary tumor challenge, then divided into five groups (n=6), which respectively received administration of PBS as the control group, free Endostar (FE) at a daily dose of 2 mg/kg based on clinical dosing, EH (only one dose of 42 mg/kg Endostar), TCLN (the TCL dose of 200 μg/mice), EH/TCLN (the same dose with that of EH and TCLN). The mice were s.c. vaccinated three times on day 4, 11 and 18. On day 7, EH were injected s.c. at the right flank. The tumor volume was calculated as 1/2× tumor length (mm)×[tumor width (mm)].[2]

In addition, animal survival study was developed using the same primary tumor challenge method as described above. Among the five groups (PBS, FE, EH, TCLN or EH/TCLN group), the survival rate of mice was observed and defined as (%) = (total number of the mice–number of the dead mice)/(total number of the mice) × 100%. On day 62 of the primary tumor challenge, the surviving mice were rechallenged with the same number of MC-38 tumor cell, and survival time of mice was monitored for another 62 days.

Analysis of T Cells and DCs in the Tumor-Bearing Mice

The vaccinated mice were sacrificed 3 days after the last immunization, and the spleen, lymph nodes and tumors were harvested and developed into single-cell suspension. The cells were then stained with appropriately diluted antibodies against CD3-PerCP/Cyanine5.5, CD8-APC, CD4-FITC, CD11c-PerCP-Cyanine5.5, MHCI-APC, MHCII-FITC and CD86-PE. T cells and DCs in the tumor-bearing mice were analyzed by flow cytometry.

T Cell Response in the Tumor-Bearing Mice

Splenocytes harvested from the tumor-bearing mice were co-cultured with MC 38 cells in a 96-well plate for 72 hours at the effector/target cell (E/T) ratios of 10:1, 20:1, 50:1, 75:1 and 100:1, respectively. CTL killing activity was determined

by CCK-8 assay (Dojindo Laboratories) according to the provided protocol. The CTL killing ratio was defined as (%) = (OD value of the control group - OD value of the experimental group)/(OD value of the control group) × 100%.

In the meantime, the concentrations of cytokine IFN-γ, IL-4 and IL-10 secreted by the splenocytes harvested from the tumor-bearing mice were determined by ELISA after stimulation with 50 μg/mL of TCL for 72 hours at 37°C.

ELISA for Immunological and Angiogenic Factors

ELISA was used to determine the levels of VEGF, MMP-9, TNF-α, IL-4, IL-6, IL-8, IL-10, IL-12 and IL-17 in the colon tumors of MC 38-bearing C57BL/6 mice. In brief, colon tumors (100 mg/sample) were lysed by adding 600 μL lysis buffer containing 20 mM sodium phosphate buffer (pH 7.4), 0.5% Triton X-100, 150 mM NaCl and 5 mM EDTA.[22] The lysate was left on ice for 30 min, then grinded, vortex-mixed and centrifuged at 14,000 g at 4 °C for 15 min. The supernatant was collected and measured by ELISA according to the manufacturer's instructions. The optical density of samples was read at 450 nm using versatile microplate readers (Varioskan Flash, Thermo Fisher Scientific, USA).

Immunohistochemistry Analysis

To estimate the microvascular content within tumor, the tumor specimen was fixed and embedded in optimal cutting temperature compound (OCT) immediately and cut into 6 μm cryopreserved-embedded tissue sections. The sections were incubated overnight with the antibody CD105 (Abcam, UK). Microvessel density (MVD) was expressed as the number of stained vessels per field, which was semi-quantified using ImageJ 1.8.0 software (Rawak Software Inc., Germany).

To observe the apoptotic cells in tumor, the tumor sections were labeled with In Situ Cell Death Detection Kit (Roche, UK) according to the provided protocol. The apoptotic cells were semi-quantified using ImageJ 1.8.0 software.

Detection of Hemoglobin Content

Drabkin reagent was employed to detect hemoglobin content in the vessels invading into the tumor. Briefly, the tumor was weighed and homogenized in 1 mL of Drabkin solution, and then centrifuged at 12,000 g for 20 minutes. The supernatant was collected and filtered through a 0.22 μm filter. Absorbance of the samples at 540 nm was measured using versatile microplate readers, and the hemoglobin content in the tumor was calculated directly from the standard curve.

Statistical Data Analysis

Data were expressed as mean ± standard deviation (SD). The differences between groups were tested using one-way ANOVA and Tukey's post-test (GraphPad Software 7.0, USA). In all comparisons, $p < 0.05$ was considered statistically significant.

Results and Discussion

Inhibition of tumor angiogenesis was first proposed as a potential strategy for tumor therapy by Folkman.[23] Endostatin has been shown to inhibit endothelial migration and proliferation in tumors, suppress angiogenesis[24] and lymphangiogenesis,[25] which in turn led to tumor cell apoptosis.[26] Huang[27] reported that anti-angiogenic-based therapy significantly reduced tumor vasculature and immune tolerance, making the tumors more vulnerable to the immune reactions. They further showed that, compared with monotherapy using anti-angiogenic factors or cytokine genes, a combination treatment of antitumor cytokine with anti-angiogenic factor-encoding genes resulted in better antitumor outcome. Zhou[28] found that ex vivo dendritic cell vaccination promoted the anti-angiogenic effect of endostatin in rat glioma. Thus, combination therapies are likely more effective by enhancing CTL activation, preventing tumor-induced immunosuppression and modulating the tumor vasculature to promote CTL infiltration.

Endostar is more stable than the naturally derived endostatin due to an additional nine amino acids at the N terminus of the protein.[11] It has been demonstrated to be able to relieve the immunosuppressive tumor microenvironment, and generate stronger antitumor immune response when used together with antigen-pulsed DC-T cells.[13]

To avoid the systemic toxicity and elevate the bioavailability of Endostar, alginate hydrogel (AH) was selected to achieve sustained release of Endostar. EH with different alginate concentrations (2.25–3%, wt/v) was fabricated. As shown in Table 1, the EE of EH was higher than 91% when the concentrations of alginate were in the range of 2.25–2.75%. The EE showed significant decrease in EH with concentration of 3%. The EC of EH declined with the increase in alginate concentration. These

Table 1 The Endostar EE and EC in the Alginate Hydrogel

AH Concentration (%)	2.25	2.5	2.75	3
EE (%)	91.7±5.31	91.3±3.60	91.8±3.11	77.9±5.30
EC (μg/mg)	157.6±2.47	145.5±2.44	136.3±1.36	102.1±2.54
Ca^{2+} concentration (wt%)	0.064	0.067	0.071	0.072

Notes: EE = (amount of the encapsulated Endostar/total amount of Endostar) × 100%. EC = weight of the encapsulated Endostar (μg)/weight of the EH (mg).

results implied that Endostar was not encapsulated well when alginate concentration was 3%, while lower alginate concentrations were more convenient for Endostar encapsulation. As shown in Table 1 and Figure 1A–C, the SEM images showed that the micropore size inside the hydrogel can be reduced by increasing the Ca^{2+} concentration within the gel. An increase of the alginate concentration induces denser packing of polymer chains in the hydrogel (Figure 1D). This may because that the high Ca^{2+} and alginate concentration significantly enhanced the mechanical properties of the hydrogel. Indeed, as we have observed, the 3% alginate hydrogel was non-injectable, while the rest three hydrogels with lower alginate concentrations were all injectable.

As illustrated in Figure 2A, a moderate burst release was observed from the 3% EH (26.36%±0.78%) on the first day due to its not well encapsulation, whereas the burst release rate of 2.75% EH was the lowest (17.26%±0.97%). The cumulative release rate reached to a plateau at day 21. On the 27th day, the final cumulative release rate of the 2.75% EH was the highest (79.6%±0.24%), slightly higher than that of the 3% EH (79.11±0.24%), thus the 2.75% EH was selected for subsequent experiments.

In vivo release of Endostar from EH was evaluated in rats, and the results illustrated in Figure 2B demonstrated a sustained release up to 26 days, wherein the effective drug concentration ranged from 105.01 ng/mL to 358.68 ng/mL was reached at day 1 and maintained until day 25. Wu[29] reported a similar Endostar level in rat plasma released from Endostar-loaded PLGA microspheres, which is shown to be as effective as FE in suppressing tumor growth, which indirectly implicated that sustained release of Endostar via delivery systems such as AH could be more effective for antitumor therapy.

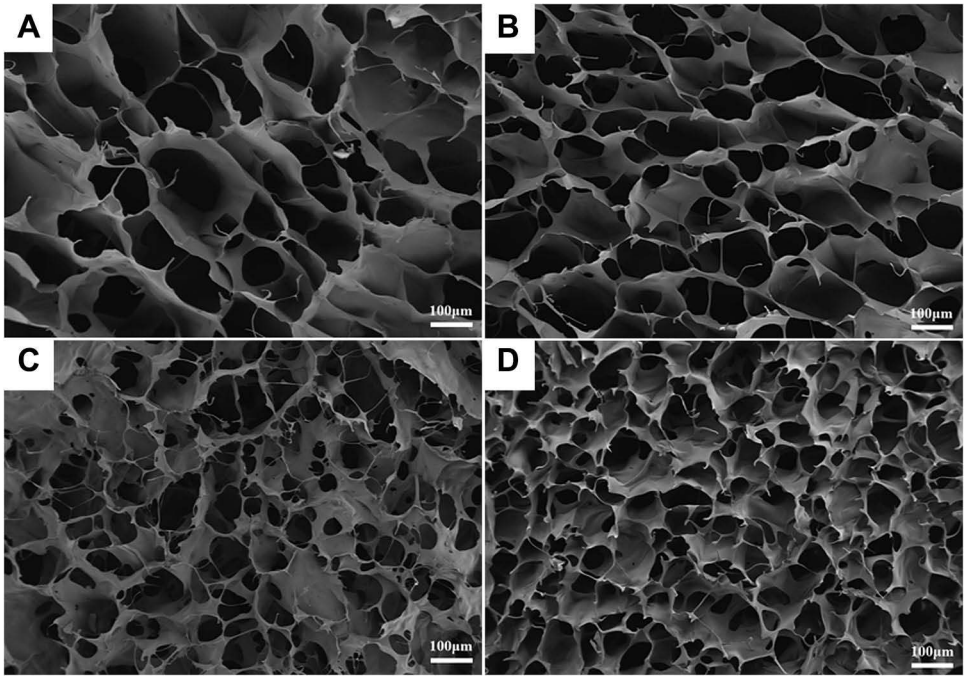

Figure 1 SEM images of alginate hydrogels at the concentration of 2.25% (**A**), 2.5% (**B**), 2.75% (**C**) and 3% (**D**).

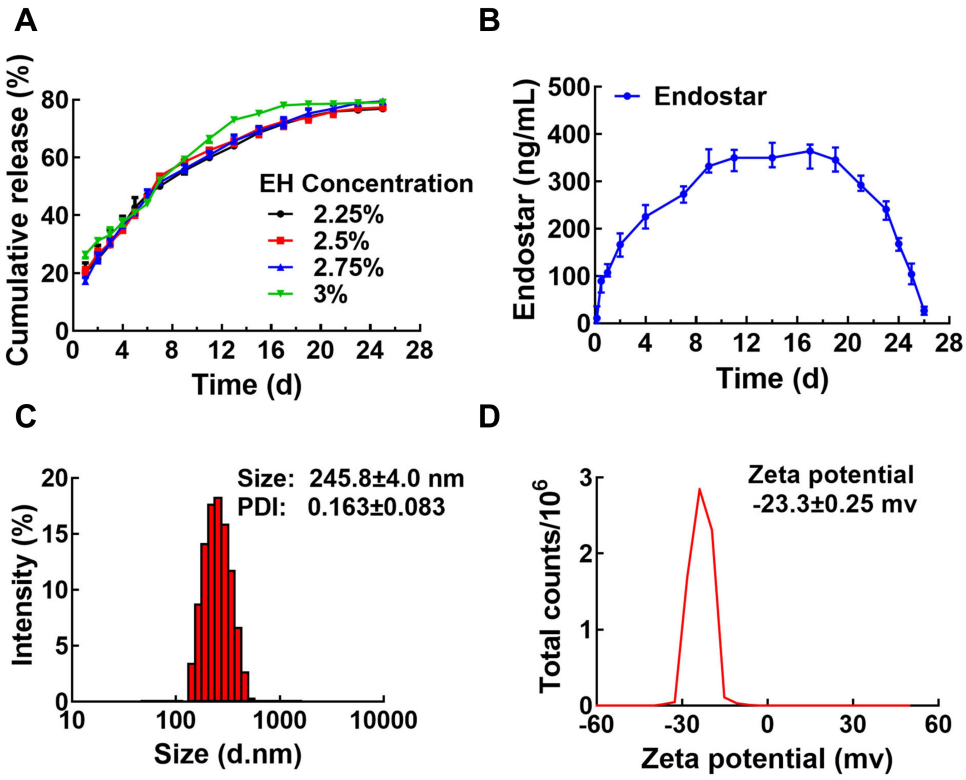

Figure 2 The Endostar release from EH and the characterization of TCLNs. (**A**) In vitro Endostar release from EH (n=4). (**B**) The concentration of Endostar in rat plasma (n=7). The distribution of DLS size (**C**) and Zeta potential (**D**) of TCLN. Polydispersity was abbreviated as PDI. The data shown were mean ± SD. (n=6).

As shown in Figure 2C and D, the characterization of TCLNs was similar to the previous results.[14] In addition, our previous study showed that PDA nanoparticles and TCLN were essentially non-cytotoxic. In the current study, the cytotoxicity of AH, AH/PDA and EH/TCLN was evaluated in NIH 3T3 cells, and the result shown in Supplementary Figure 1 demonstrates excellent cytocompatibility of AH, AH/PDA and EH/TCLN.

Tumor-bearing mice were employed to evaluate the antitumor effect of EH/TCLN. After optimization, the dose of TCLN was 200 μg per mouse, which was lower than the applied dosage in our previous report (300 μg per mouse).[14] As shown in Figure 3A–C, EH/TCLN demonstrated the strongest antitumor effect with a tumor inhibition rate (IR) of 92.3% at day 21 after tumor challenge, which was significantly higher than the PBS, FE and TCLN treatment groups. No significant difference in body weight was observed among all groups, indicating no evident adverse effect of all treatments (Supplementary Figure 2).

Although there was no significant difference of the antitumor effect between the EH and EH/TCLN groups, the respective survival results of the EH and EH/TCLN groups showed evident variation. As shown in Figure 3D, TCLN/EH treatment led to complete tumor regression with a 62.5% survival rate for 62 days. In contrast, all other groups exhibited 0% survival rate. Moreover, all the survived mice in the EH/TCLN group were tumor-free during the 62-day-period after re-challenge with contralateral tumor cells, indicating the presence of immune memory against tumor recurrence induced by the EH/TCLN treatment.

Next, the host immunity against tumor boosted by polydopamine nanovaccine combination therapy was investigated. The adaptive immune response that specifically kills tumor cells is mainly mediated by $CD8^+$ CTLs, and $CD4^+$ T helper cells that may promote the activation and proliferation of CTLs.[30] These two types of T cells in the spleen and draining lymph nodes (DLNs) were analyzed after the aforementioned treatments. As shown in Figure 4, in short, among all the groups, EH/TCLN treatment resulted in the most significant increase of both $CD8^+$ and $CD4^+$ T cell populations in both spleens and DLNs. This is consistent with its strongest antitumor effect (Figure 3). Since the dose of TCLN in this study was lower than the effective dose of TCLN (300 μg per mouse) used in our previous study,[14] T cell subpopulations in the spleens and DLNs in the TCLN treatment group reported here was not significantly different from that in the EH

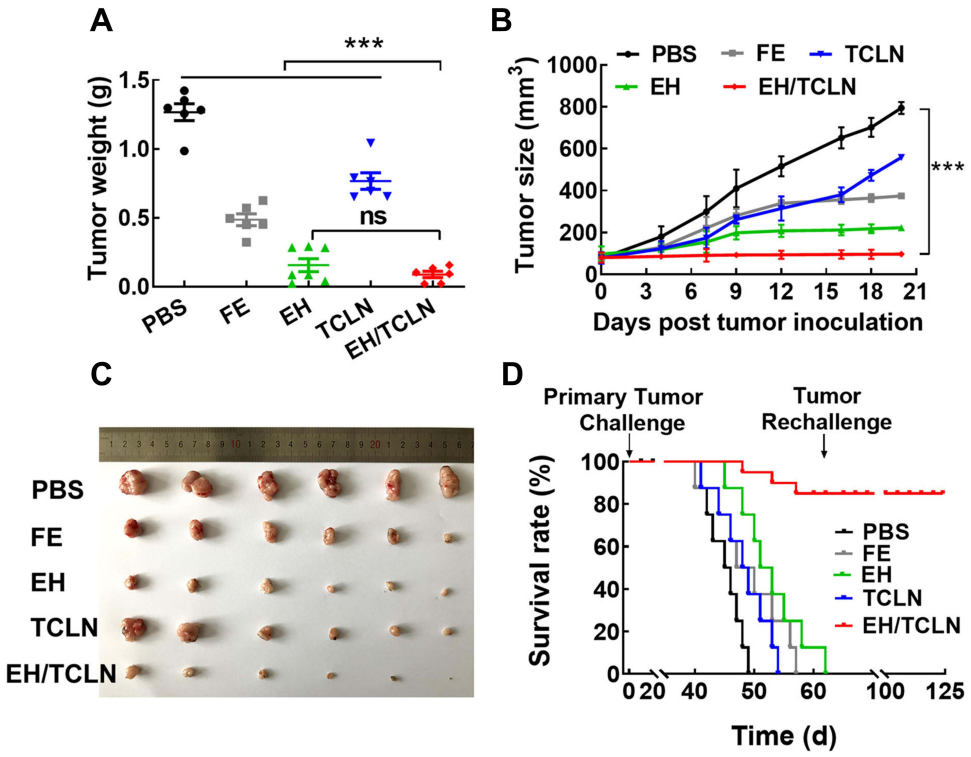

Figure 3 In vivo antitumor effect of EH/TCLN. (**A**) The tumor weight of mice on 21st day after tumor challenge. (**B**) The tumor volume during the treatment. (**C**) The picture of tumor dissected from the tumor-bearing mice. The bars shown were mean ± SD (n=6), and the differences between groups were determined using one-way ANOVA with Tukey's post-test, ***p<0.001. (**D**) The survival rate of mice in different treatment groups. (n=8).

treatment group, suggesting that its antitumor ability was not strong enough at a dose below 200 μg per mouse. Nevertheless, significantly higher percentages of both splenic $CD8^+$ and $CD4^+$ T cells were observed after TCLN treatment as compared with FE and PBS treatments. As compared with FE, the EH treatment led to the most significantly increase in both splenic $CD8^+$ and $CD4^+$ T cell percentages, with only a moderate elevation in the DLNs.

We further investigated the activity of CTLs using MC-38 tumor cells. As shown in Figure 5A, EH/TCLN treatment induced the highest cytolytic activity (76.5%) against MC-38 cells among all the groups, which further supported the strong antitumor effect of EH/TCLN, while the EH treatment led to the second highest cytolytic activity (56.6%).

The culture supernatant of spleen lymphocytes after antigen restimulation was collected for determination of cytokine production. IFN-γ, a marker cytokine for T helper 1 cells (Th1), can enhance cellular immune responses.[31] IL-4 and IL-10 are immunosuppressive cytokines secreted by T helper 2 cells (Th2).[32,33] Our data demonstrated that EH/TCLN induced the highest IFN-γ production with the lowest level of IL-4 and IL-10 quantified in all treatment groups. Level of IFN-γ was also increased in the FE, EH and TCLN groups, but to a lesser extent than that in the EH/TCLN group (Figure 5B–D).

T lymphocyte response in the tumor was also examined, and the results were displayed in Figure 6. EH/TCLN led to the most significantly increase in proportion of $CD3^+CD8^+$ T cells in the tumor among all groups, verifying their stronger ability to stimulate adaptive immune response. However, treatment with TCLN or Endostar alone moderately increased the proportion of $CD3^+CD8^+$ T cells, resulting in approximately half of the EH/TCLN group (Figure 6A). $CD4^+$ T cell analysis demonstrated a similar pattern (Figure 6B). Naive DCs (nDCs) undergo the process of maturation when stimulated with tumor antigens, and the matured DCs (mDCs) possess more powerful antigen presentation capability for $CD8^+$ T cell activation and destruction of tumor cells. The intratumoral mDCs were extracted and evaluated after the combination treatment, by labelling $CD11c^+MHCI^+$, $CD11c^+CD86^+$ as well as $CD11c^+$ $MHCII^+$ as surface markers for mDCs. As displayed in Figure 6C–E and Supplementary Figure 3, among all groups, treatment with EH/TCLN resulted in the highest percentage of matured DCs (45.3% of $MHCI^+$ and 28.6% of $MHCII^+$), while treatment with EH alone led

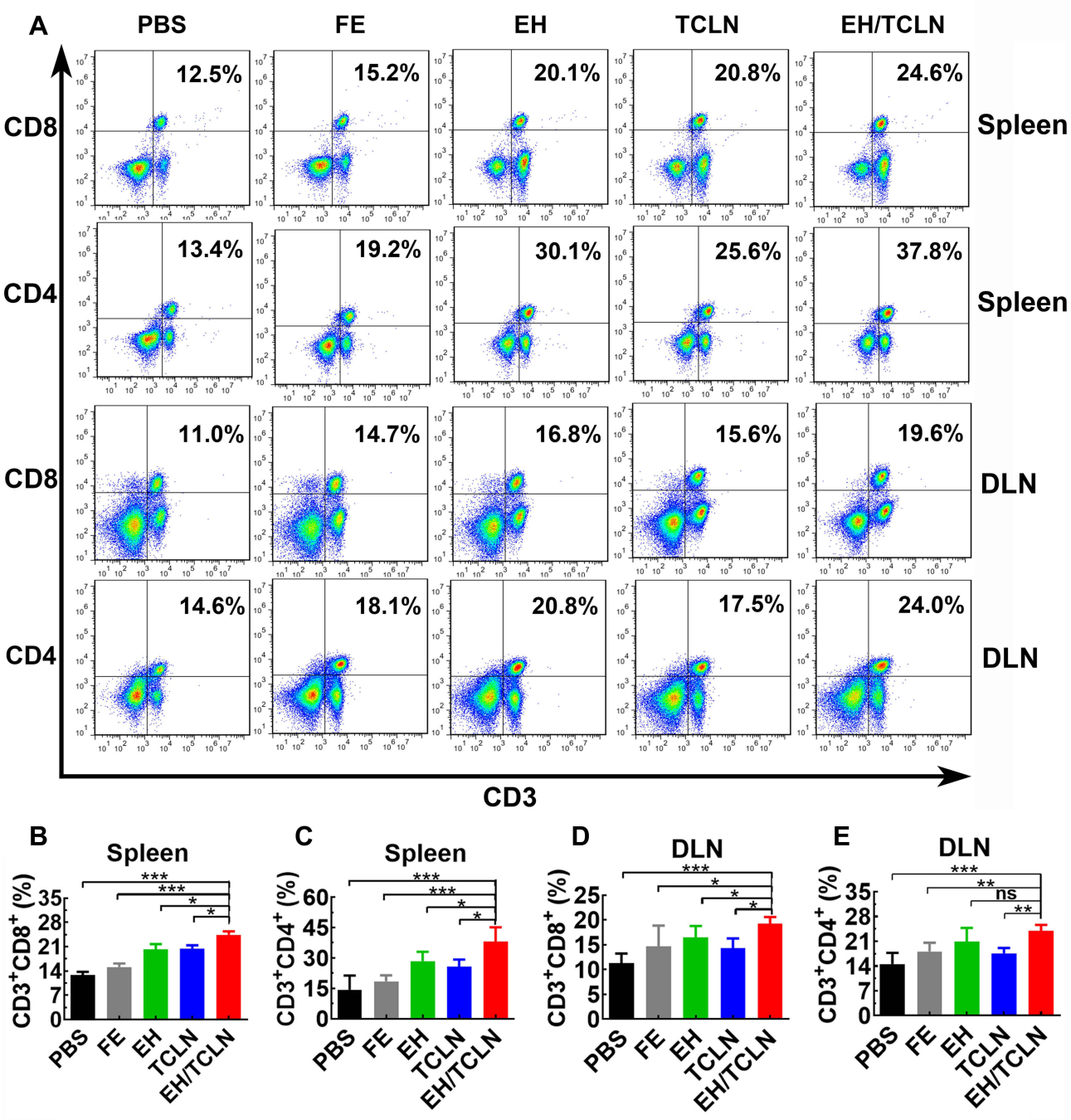

Figure 4 The effect of EH/TCLN on T cells in colon tumor-bearing mice. Phenotypic analysis of $CD3^+CD8^+$ (the first row of **A** and **B**) and $CD3^+CD4^+$ (the second row of **A** and **C**) T cells in spleen at 21 days after tumor cell inoculation. Phenotypic analysis of $CD3^+CD8^+$ (the third row of **A** and **D**) and $CD3^+CD4^+$ T cells (the fourth row of **A** and **E**) in DLN at 21 days after tumor cell inoculation. The bars shown were mean ± SD (n=6), and the differences between groups were determined using one-way ANOVA with Tukey's post-test, *p<0.05, **p<0.01, ***p<0.001, ns = not statistically significant.

to a moderate increase in matured DCs number (32.1% of $MHCI^+$ and 23.9% of $MHCII^+$). These results indicated that EH/TCLN treatment was in favor of nDC maturation that would assist efficient antigen presentation.

Suppression against antitumor immune activities is one of the major characteristics of tumor microenvironment. Tumor microenvironment-related cytokines (TMCs) were also detected after combination treatments because they protect tumor cells, maintain the tumor microenvironment and inhibit the activity of CTLs. As a result, TMCs play a crucial role in tumor development. IL-4,[34] IL-6,[35] IL-10, IL-17[30,36] and TNF-α,[37,38] as the TMCs reported in the most studies, may be effective in colon tumor progression. Moreover, IL-8 has also been proven to play an important role in tumor growth,

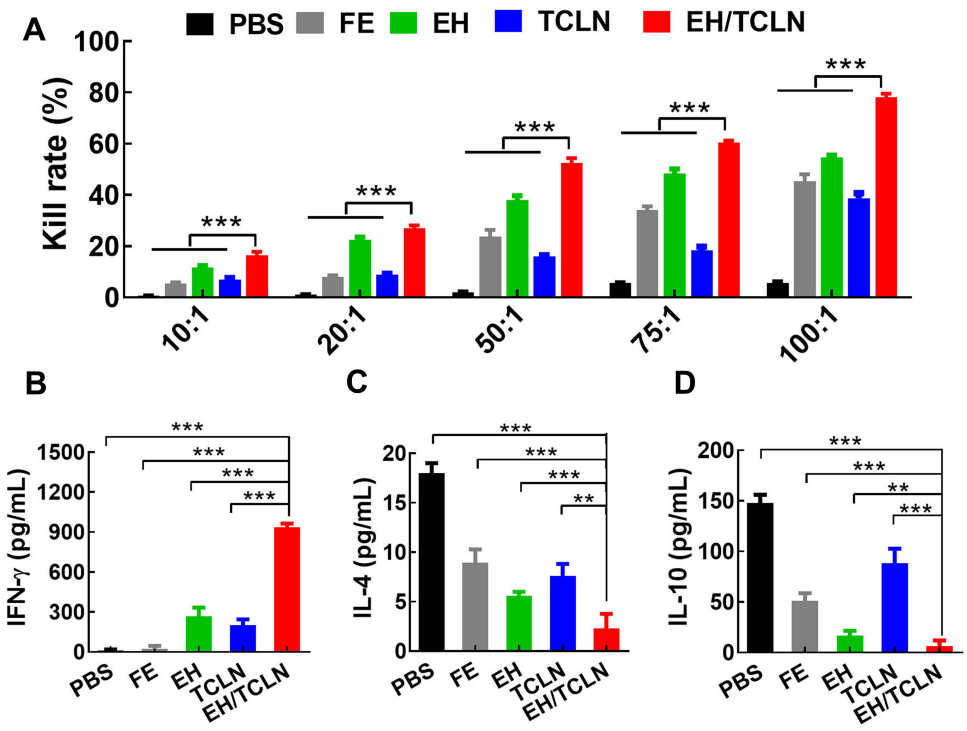

Figure 5 The effect of the EH/TCLN treatment on T cell function in colon tumor-bearing mice. (**A**) The killing activity of the T cells. The production of IFN-γ (**B**), IL-4 (**C**) and IL-10 (**D**) in the spleen cell culture supernatants. The bars shown were mean ± SD (n=6), and the differences between groups were determined using one-way ANOVA with Tukey's post-test, **p<0.01, ***p<0.001.

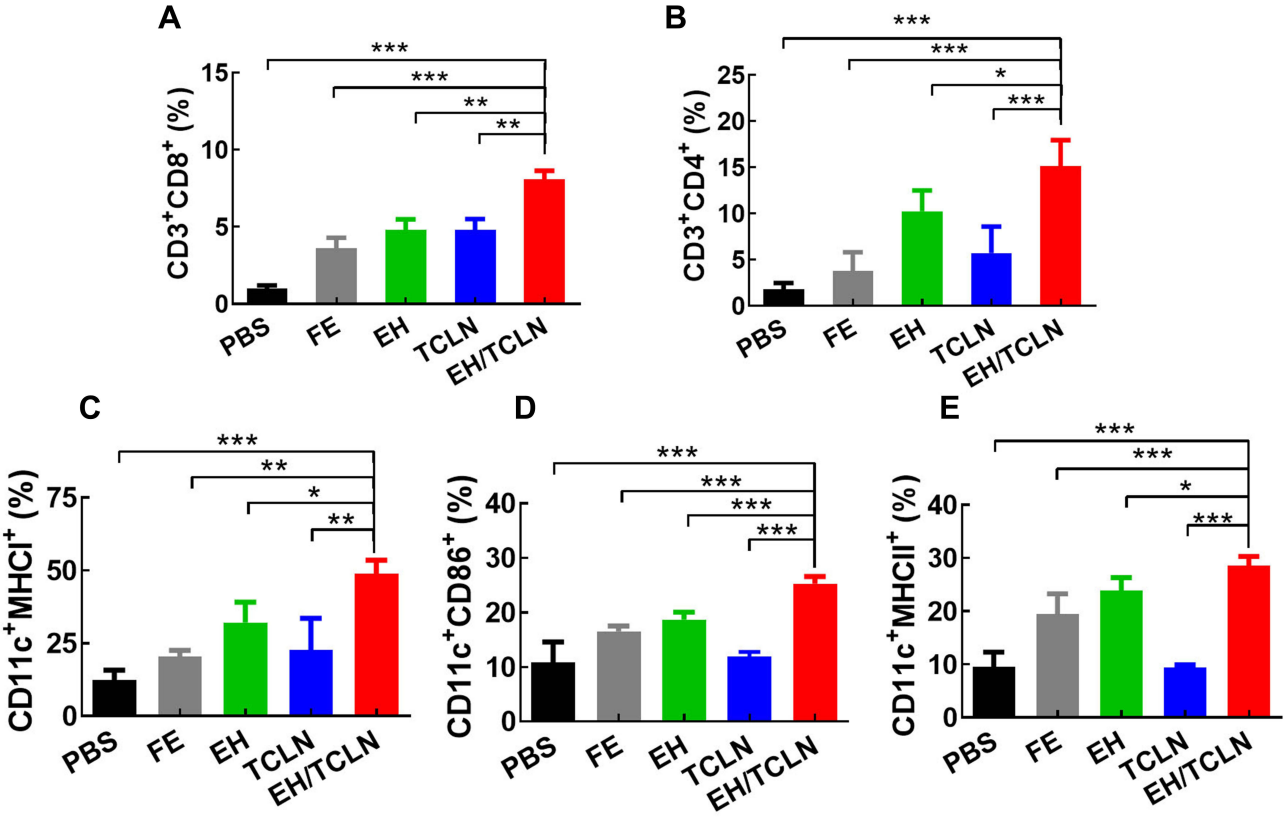

Figure 6 Intratumoral analysis of $CD3^+CD8^+$ cells (**A**), $CD3^+CD4^+$ cells (**B**) and $CD11c^+MHCI^+$ cells (**C**), $CD11c^+CD86^+$ cells (**D**) and $CD11c^+$ $MHCII^+$ cells (**E**). The bars shown were mean ± SD (n=6), and the differences between groups were determined using one-way ANOVA with Tukey's post-test, *p<0.05, **p<0.01, ***p<0.001.

angiogenesis, and metastasis.[39] In addition, IL-12 is one of the most commonly examined antitumor cytokine,[40,41] having been reported in a number of preclinical animal models for its use to elicit the host immune responses against tumor,[42] while inhibiting intratumoral MMP-9 and VEGF levels.[43]

Hence, the TMCs were analyzed to better understand the mechanism underlying the antitumor effect of the EH/TCLN combination therapy. For this purpose, the levels of IL-4, IL-6, IL-8, IL-10, IL-12, IL-17, and TNF-α in the tumor lysate were tested by ELISA. As shown in Figure 7, EH/TCLN treatment led to the most significantly elevation of IL-12 among all groups. In addition, it substantially decreased TMCs such as IL-4, IL-6, IL-8, IL-10, IL-17 and TNF-α, which have been shown to participate in tumor growth. Similar trend was also observed in the EH group, but with a lower extent in comparison to that in the EH/TCLN group. These data indicated that EH/TCLN treatment caused major changes in the tumor immuno-micro-environment, which might explain why the tumor growth was significantly suppressed in this group (Figure 3).

Pro-angiogenesis is a critical factor affecting tumor microenvironment. Angiogenic stimulators secreted by tumor cells induced the growth of blood vasculature to supply oxygen and nutrition for tumor progression, invasion and metastasis. Tumor-derived VEGF not only plays a key role in angiogenesis[44] but also could impair DC function and maturation, increase programmed cell death ligand 1(PDL1) expression by DCs, and block T cell activation.[45] Recent reports showed that VEGF could not function properly without matrix metalloproteinases, MMP-9 in particular,[46] which are produced by intratumoral stroma.[47]

The levels of VEGF and MMP-9 in the tumors were tested after the aforementioned treatments. As shown in Figure 8A and B, EH/TCLN significantly reduced the levels of both VEGF and MMP-9 in the tumors as compared with the other four groups. VEGF levels were moderately decreased in the FE or EH group, while VEGF level in the TCLN group was slightly decreased compared with the control group. MMP-9 level in the FE, EH or TCLN group was reduced by approximately 20% as compared with the control group. These results indicated that TCLN treatment did not exert evident inhibitory effect on intratumoral angiogenesis, which could partly explain why the mice treated with TCLN alone had the larger tumor size than the other treatment groups. The EH/TCLN led to dramatically decrease of VEGF and MMP-9, thereby significantly inhibited tumor angiogenesis.

In addition to VEGF and MMP-9, multiple cell types with established roles in immune-suppression have been shown to promote angiogenesis within the tumor microenvironment through the production of various growth factors.[48] TMCs such as IL-

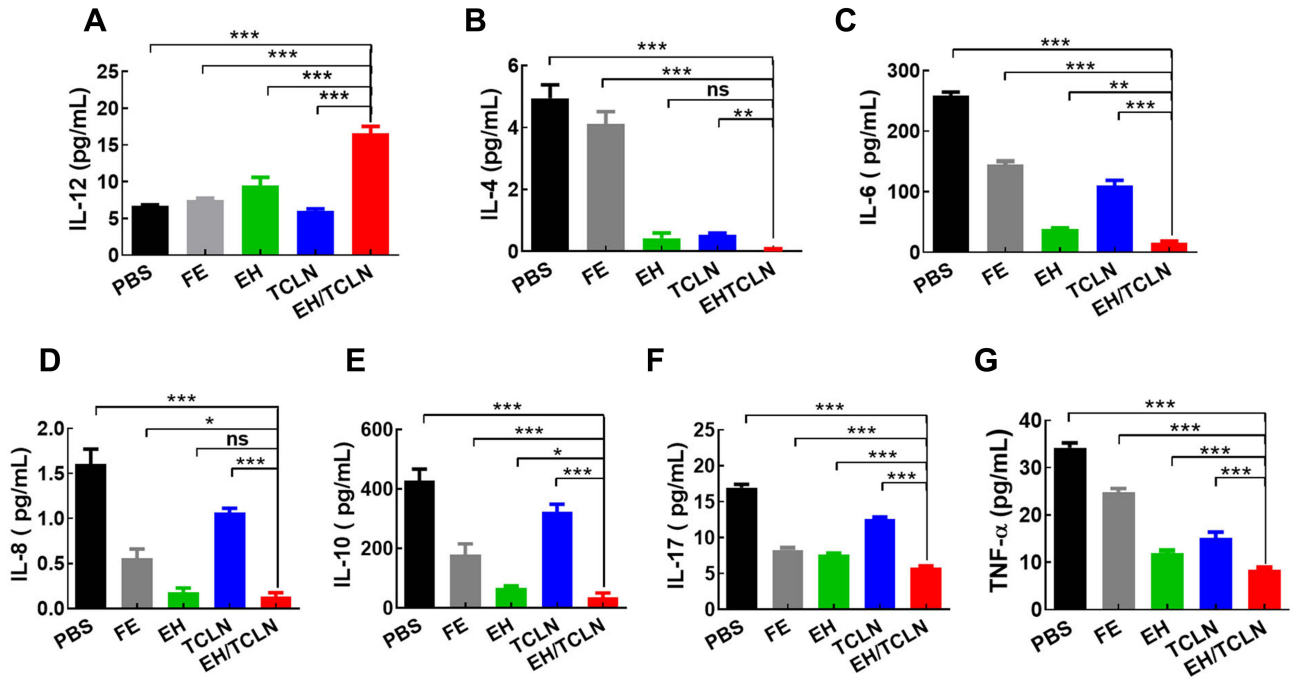

Figure 7 Analysis of intratumoral IL-12 (**A**), IL-4 (**B**), IL-6 (**C**), IL-8 (**D**), IL-10 (**E**), IL-17 (**F**), and TNF-α (**G**) after combination treatment. The bars shown were mean ± SD (n=6), and the differences between groups were determined using one-way ANOVA with Tukey's post-test, *p<0.05, **p<0.01, ***p<0.001, ns = not statistically significant.

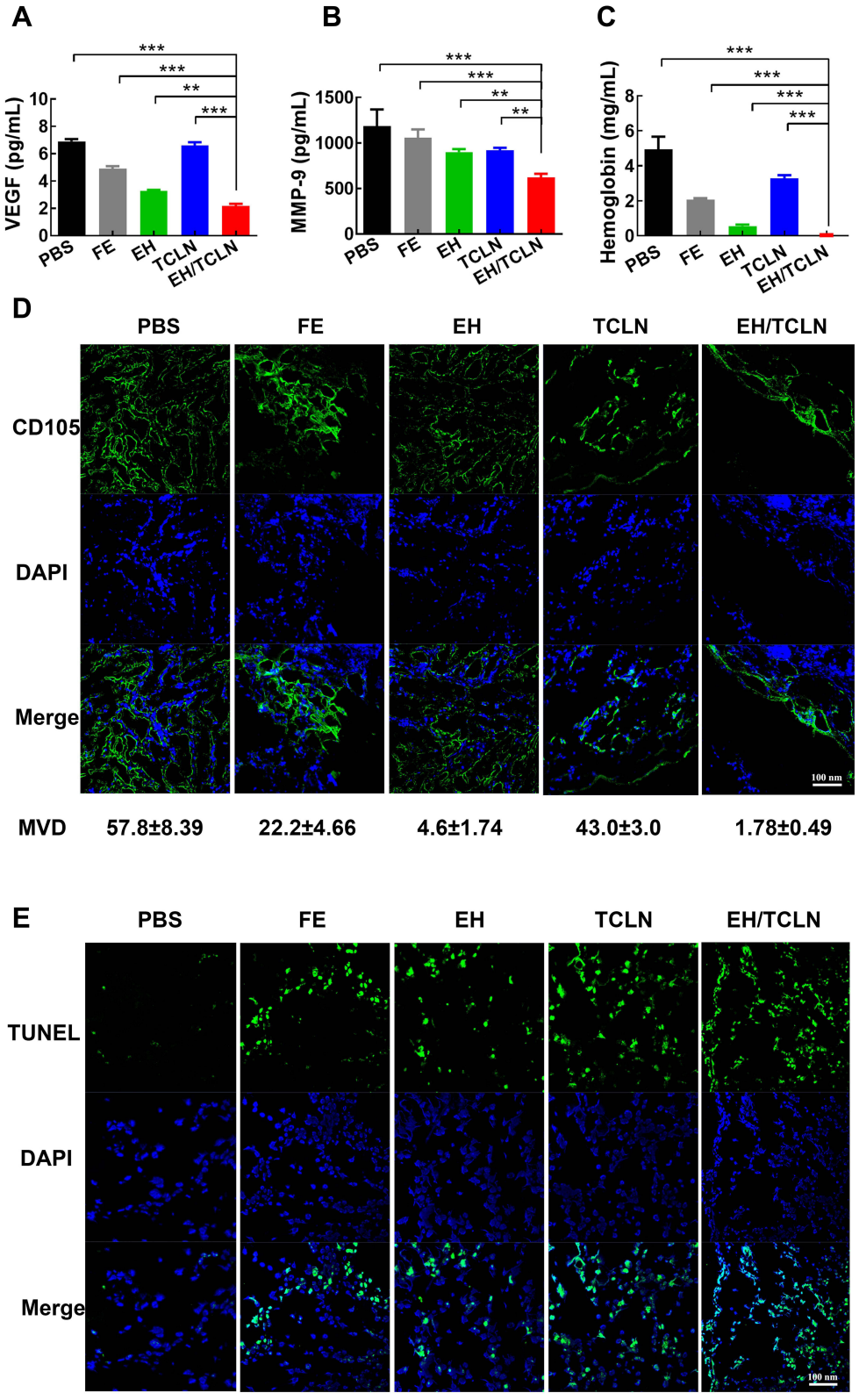

Figure 8 In vivo anti-angiogenesis effect of EH/TCLN. Levels of intratumoral VEGF (**A**) and MMP-9 (**B**). (**C**) Intratumoral hemoglobin content. Fluorescence immunohistochemistry for neo-vascular marker CD105 (**D**) and apoptosis test in the tumor sections (**E**). The bars shown were mean ± SD (n=6), and the differences between the groups were determined using one-way ANOVA with Tukey's post-test, **p<0.01, ***p<0.001.

4, IL-6, IL-8, IL-10, IL-17 and TNF-α were secreted by immunosuppressive cells such as tumor associated macrophages, T helper cell 17 and myeloid-derived suppressor cells, which promote tumor angiogenesis and tumor revascularization as pro-angiogenic growth factors.[48] Although IL-12 was able to inhibit the growth of tumor vessels, it was negatively regulated by cytokines such as IL-4 and IL-10.[40] Our results were consistent with previous reports, providing further support for the markedly enhanced anti-angiogenic activity of the EH/TCLN therapy. On the other hand, the anti-angiogenic data showed the superiority of EH over FE by altering the route and mode of administration, exhibiting the advantage of controlled-release hydrogel as a drug delivery material compared with the free drug.

We further determined the hemoglobin content and MVD within the tumors to investigate the effect of the combination treatment on intratumoral angiogenesis. As shown in Figure 8C and D, both intratumoral hemoglobin content and MVD in the EH/TCLN group were the lowest (with the control group showing the highest and other groups following the order of EH <TCLN). The data illustrated that EH/TCLN reduced hemoglobin content and MVD by 99.4% and 97%, respectively, as compared with the control group. This observation was consistent with the results of the studies on angiogenic stimulators (Figures 7, 8A and B), and further verified the anti-angiogenic effect of the EH/TCLN treatment, which contribute to its comparatively more superior antitumor effect shown as the smallest tumor size (Figure 3B) and tumor regression (Figure 3D) observed in mice treated with EH/TCLN.

Furthermore, it has been previously reported that endostatin induced tumor cell apoptosis partly due to the loss of adequate vasculature.[26] In this study, tumor apoptotic cells were also quantified and observed by using the TUNEL assay. The number of apoptotic cells in the EH/TCLN group was significantly higher than that in the other groups (Figure 8E).

Based on the pro-angiogenic analysis, EH/TCLN reduced VEGF expression by more than three folds and MMP-9 expression by two folds as compared with the control group, leading to the lowest MVD and hemoglobin content among all groups, implying that intratumoral supplementary of oxygen and nutrition was dramatically limited by EH/TCLN treatment, finally resulting in the highest apoptotic rate (74.2±3.35%).

In summary, our data showed that the EH/TCLN could substantially down-regulate the TMCs including IL-4, 6, 8, 10, 17 and TNF-α, while elevating the production of immunostimulatory cytokine IL-12, thereby creating a favorable immune context for the induction of antitumor immunity. It also significantly increased the number of $CD8^+$ and $CD4^+$ T cells in the spleen, draining lymph nodes and tumors, enhanced the maturation of DCs and specific lytic activity of CTL, and hence eliciting outstanding antitumor immune response. Moreover, treatment with EH/TCLN inhibited the intratumoral angiogenesis, which further contribute to induction of antitumor immunity.

It was worth mentioning that sustained-release delivery system also achieved good efficacy.[29,49] Free Endostar with high dosages (15 mg/kg/day)[12,13] and Endostar alginate hydrogel (2 mg/kg/day for 25 days) in our previous research showed that Endostar not only reversed the immunosuppressive tumor microenvironment but also improved the antitumor immune response. This study further demonstrated that sustained release of Endostar could improve the therapeutic efficacy and achieve a good immune activating effect. However, EH treatment alone could not substantially improve the survival rate of mice. This may be due to the fact that the anti-angiogenic treatment could induce drug resistance of the tumor via a variety of mechanisms,[50,51] which ultimately led to recurrence of tumors.

It is possible that tumor development proceeds by the co-option of the homeostatic tissue repair programming that promotes concurrent angiogenesis and immunosuppression, which in turn work hand-in-hand within the tumor microenvironment.[45] Activation of antitumor immune response needs to overcome the immunosuppressive barrier that is imposed by immunosuppressive immune cells and cytokines. EH/TCLN treatment reported in the present study not only tremendously inhibited the tumor angiogenesis but also significantly enhanced the antitumor immunity responses, showing a high degree of synergy and verifying the inevitable link between active immunotherapy and anti-angiogenic therapy.

Conclusions

The ultimate aim of this study was to investigate whether TCLN nanovaccine, when applied in combination with anti-angiogenic agent, would generate synergistic antitumor efficacy. For this purpose, EH/TCLN loaded with a dose of 42 mg/kg Endostar was fabricated, which was demonstrated to be essentially non-cytotoxic with satisfying sustained in vivo release profiles. EH/TCLN, was demonstrated to significantly suppress tumor growth and prolong the survival time of the tumor-bearing mice. Further studies indicated that EH/TCLN successfully improved the tumor microenvironment by promoting the

maturation and antigen presentation of DC cells, activating the antitumor T cell immunity and inhibiting tumor angiogenesis. Our data suggested that EH/TCLN might be a potential combination strategy for treatment against colon tumor.

Acknowledgments

This research was funded by the National Natural Science Foundation of China (31300794, 31771097, and 81972899), Natural Science Foundation of Tianjin City (16JCZDJC35800), CAMS Innovation Fund for Medical Sciences (2017-I2M-1-016 and 2021-I2M-1-058), the Non-profit Central Research Institute Fund of the Chinese Academy of Medical Sciences(2021-JKCS-002), and Specific Program for High-Tech Leader & Team of Tianjin Government.

Disclosure

The authors report no conflicts of interest in this work.

References

1. Park CG, Hartl CA, Schmid D, Carmona EM, Kim HJ, Goldberg MS. Extended release of perioperative immunotherapy prevents tumor recurrence and eliminates metastases. *Sci Transl Med*. 2018;10:433. doi:10.1126/scitranslmed.aar1916
2. Goldberg MS. Improving cancer immunotherapy through nanotechnology. *Nat Rev Cancer*. 2019;19(10):587–602. doi:10.1038/s41568-019-0186-9
3. Yarchoan M, Hopkins A, Jaffee EM. Tumor mutational burden and response rate to PD-1 inhibition. *N Engl J Med*. 2017;377(25):2500–2501. doi:10.1056/NEJMc1713444
4. Shi GN, Zhang CN, Xu R, et al. Enhanced antitumor immunity by targeting dendritic cells with tumor cell lysate-loaded chitosan nanoparticles vaccine. *Biomaterials*. 2017;113:191–202. doi:10.1016/j.biomaterials.2016.10.047
5. Hu X, Wu T, Qin X, et al. Tumor lysate-loaded lipid hybrid nanovaccine collaborated with an immune checkpoint antagonist for combination immunotherapy. *Adv Healthc Mater*. 2019;8(1):e1800837. doi:10.1002/adhm.201800837
6. Wang J, Wang S, Ye T, et al. Choice of nanovaccine delivery mode has profound impacts on the intralymph node spatiotemporal distribution and immunotherapy efficacy. *Adv Sci*. 2020;7(19):2001108. doi:10.1002/advs.202001108
7. Wang H, Mooney DJ. Biomaterial-assisted targeted modulation of immune cells in cancer treatment. *Nat Mater*. 2018;17(9):761–772. doi:10.1038/s41563-018-0147-9
8. Jayson GC, Kerbel R, Ellis LM, Harris AL. Antiangiogenic therapy in oncology: current status and future directions. *Lancet*. 2016;388 (10043):518–529. doi:10.1016/S0140-6736(15)01088-0
9. Tartour E, Pere H, Maillere B, et al. Angiogenesis and immunity: a bidirectional link potentially relevant for the monitoring of antiangiogenic therapy and the development of novel therapeutic combination with immunotherapy. *Cancer Metastasis Rev*. 2011;30(1):83–95. doi:10.1007/s10555-011-9281-4
10. Bhattarai P, Hameed S, Dai Z. Recent advances in anti-angiogenic nanomedicines for cancer therapy. *Nanoscale*. 2018;10(12):5393–5423. doi:10.1039/C7NR09612G
11. Luo Y, Zhou B; Inventors; Yantai Rongchang Biotechnology Co., Ltd., assignee. Endostatin producing process. China patent CN1324818. 2001 May 12.
12. Liu X, Nie W, Xie Q, et al. Endostatin reverses immunosuppression of the tumor microenvironment in lung carcinoma. *Oncol Lett*. 2018;15 (2):1874–1880. doi:10.3892/ol.2017.7455
13. Liang J, Liu X, Xie Q, et al. Endostatin enhances antitumor effect of tumor antigen-pulsed dendritic cell therapy in mouse xenograft model of lung carcinoma. *Chin J Cancer Res*. 2016;28(4):452–460. doi:10.21147/j.issn.1000-9604.2016.04.09
14. Wang X, Wang N, Yang Y, et al. Polydopamine nanoparticles carrying tumor cell lysate as a potential vaccine for colorectal cancer immunotherapy. *Biomater Sci*. 2019;7(7):3062–3075. doi:10.1039/C9BM00010K
15. Kapishon V, Whitney RA, Champagne P, Cunningham MF, Neufeld RJ. Polymerization induced self-assembly of alginate based amphiphilic graft copolymers synthesized by single electron transfer living radical polymerization. *Biomacromolecules*. 2015;16(7):2040–2048. doi:10.1021/acs.biomac.5b00470
16. He L, Shang Z, Liu H, Yuan ZX, Murgia S. Alginate-based platforms for cancer-targeted drug delivery. *Biomed Res Int*. 2020;2020:1487259. doi:10.1155/2020/1487259
17. Abasalizadeh F, Moghaddam SV, Alizadeh E, et al. Alginate-based hydrogels as drug delivery vehicles in cancer treatment and their applications in wound dressing and 3D bioprinting. *J Biol Eng*. 2020;14:8. doi:10.1186/s13036-020-0227-7
18. Chen W, Hu S. Suitable carriers for encapsulation and distribution of endostar: comparison of endostar-loaded particulate carriers. *Int J Nanomedicine*. 2011;6:1535–1541. doi:10.2147/IJN.S21881
19. Wang X, Jiang Z, Shi J, et al. Dopamine-modified alginate beads reinforced by cross-linking via titanium coordination or self-polymerization and its application in enzyme immobilization. *Ind Eng Chem Res*. 2013;52(42):14828–14836. doi:10.1021/ie401239e
20. Desai RM, Koshy ST, Hilderbrand SA, Mooney DJ, Joshi NS. Versatile click alginate hydrogels crosslinked via tetrazine-norbornene chemistry. *Biomaterials*. 2015;50:30–37. doi:10.1016/j.biomaterials.2015.01.048
21. Zhang Y, Li X, Zhong N, Huang Y, He K, Ye X. Injectable in situ dual-crosslinking hyaluronic acid and sodium alginate based hydrogels for drug release. *J Biomater Sci Polym Ed*. 2019;30(12):995–1007. doi:10.1080/09205063.2019.1618546
22. Xu Q, Gu J, Lv Y, et al. Angiogenesis for tumor vascular normalization of Endostar on hepatoma 22 tumor-bearing mice is involved in the immune response. *Oncol Lett*. 2018;15(3):3437–3446. doi:10.3892/ol.2018.7734
23. Folkman J. Tumor angiogenesis: therapeutic implications. *N Engl J Med*. 1971;285(21):1182–1186. doi:10.1056/NEJM197111182852108
24. O'Reilly MS, Pirie-Shepherd S, Lane WS, Folkman J. Antiangiogenic activity of the cleaved conformation of the serpin antithrombin. *Science*. 1999;285(5435):1926–1928. doi:10.1126/science.285.5435.1926
25. Zhuo W, Chen Y, Song X, Luo Y. Endostatin specifically targets both tumor blood vessels and lymphatic vessels. *Front Med*. 2011;5(4):336–340. doi:10.1007/s11684-011-0163-5

26. Wang L, Yao B, Li Q, et al. Gene therapy with recombinant adenovirus encoding endostatin encapsulated in cationic liposome in coxsackievirus and adenovirus receptor-deficient colon carcinoma murine models. *Hum Gene Ther*. 2011;22(9):1061–1069. doi:10.1089/hum.2011.014
27. Huang KW, Wu HL, Lin HL, et al. Combining antiangiogenic therapy with immunotherapy exerts better therapeutical effects on large tumors in a woodchuck hepatoma model. *Proc Natl Acad Sci U S A*. 2010;107(33):14769–14774. doi:10.1073/pnas.1009534107
28. Zhou X, Liao Y, Li H, Zhao Z, Liu Q. Dendritic cell vaccination enhances antiangiogenesis induced by endostatin in rat glioma. *J Cancer Res Ther*. 2016;12(1):198–203. doi:10.4103/0973-1482.151430
29. Wu J, Ding D, Ren G, Xu X, Yin X, Hu Y. Sustained delivery of endostatin improves the efficacy of therapy in Lewis lung cancer model. *J Control Release*. 2009;134(2):91–97. doi:10.1016/j.jconrel.2008.11.004
30. Schreiber RD, Old LJ, Smyth MJ. Cancer immunoediting: integrating immunity's roles in cancer suppression and promotion. *Science*. 2011;331(6024):1565. doi:10.1126/science.1203486
31. Sojka DK, Fowell DJ. Regulatory T cells inhibit acute IFN-γ synthesis without blocking T-helper cell type 1 (Th1) differentiation via a compartmentalized requirement for IL-10. *Proc Natl Acad Sci U S A*. 2011;108(45):18336–18341. doi:10.1073/pnas.1110566108
32. Marinaro M, Staats HF, Hiroi T, et al. Mucosal adjuvant effect of cholera toxin in mice results from induction of T helper 2 (Th2) cells and IL-4. *J Immunol*. 1995;155(10):4621–4629.
33. Mollazadeh H, Cicero AFG, Blesso CN, Pirro M, Majeed M, Sahebkar A. Immune modulation by curcumin: the role of interleukin-10. *Crit Rev Food Sci Nutr*. 2019;59(1):89–101. doi:10.1080/10408398.2017.1358139
34. Todaro M, Alea MP, Di Stefano AB, et al. Colon cancer stem cells dictate tumor growth and resist cell death by production of interleukin-4. *Cell Stem Cell*. 2007;1(4):389–402. doi:10.1016/j.stem.2007.08.001
35. Huang YJ, Yang CK, Wei PL, et al. Ovatodiolide suppresses colon tumorigenesis and prevents polarization of M2 tumor-associated macrophages through YAP oncogenic pathways. *J Hematol Oncol*. 2017;10(1):60. doi:10.1186/s13045-017-0421-3
36. Briukhovetska D, Dörr J, Endres S, Libby P, Dinarello CA, Kobold S. Interleukins in cancer: from biology to therapy. *Nat Rev Cancer*. 2021;21(8):481–499. doi:10.1038/s41568-021-00363-z
37. Kathania M, Khare P, Zeng M, et al. Itch inhibits IL-17-mediated colon inflammation and tumorigenesis by ROR-γt ubiquitination. *Nat Immunol*. 2016;17(8):997–1004. doi:10.1038/ni.3488
38. Sharp SP, Avram D, Stain SC, Lee EC. Local and systemic Th17 immune response associated with advanced stage colon cancer. *J Surg Res*. 2017;208:180–186. doi:10.1016/j.jss.2016.09.038
39. Mizukami Y, Jo WS, Duerr EM, et al. Induction of interleukin-8 preserves the angiogenic response in HIF-1alpha-deficient colon cancer cells. *Nat Med*. 2005;11(9):992–997. doi:10.1038/nm1294
40. Tugues S, Burkhard SH, Ohs I, et al. New insights into IL-12-mediated tumor suppression. *Cell Death Differ*. 2015;22(2):237–246. doi:10.1038/cdd.2014.134
41. Tait Wojno ED, Hunter CA, Stumhofer JS. The immunobiology of the interleukin-12 family: room for discovery. *Immunity*. 2019;50(4):851–870. doi:10.1016/j.immuni.2019.03.011
42. Mansurov A, Ishihara J, Hosseinchi P, et al. Collagen-binding IL-12 enhances tumour inflammation and drives the complete remission of established immunologically cold mouse tumours. *Nat Biomed Eng*. 2020;4(5):531–543. doi:10.1038/s41551-020-0549-2
43. Scott KA, Holdsworth H, Balkwill FR, Dias S. Exploiting changes in the tumour microenvironment with sequential cytokine and matrix metalloprotease inhibitor treatment in a murine breast cancer model. *Br J Cancer*. 2000;83(11):1538–1543. doi:10.1054/bjoc.2000.1487
44. Kong D-H, Kim MR, Jang JH, Na H-J, Lee S. A review of anti-angiogenic targets for monoclonal antibody cancer therapy. *Int J Mol Sci*. 2017;18(8):1786. doi:10.3390/ijms18081786
45. Motz GT, Coukos G. The parallel lives of angiogenesis and immunosuppression: cancer and other tales. *Nat Rev Immunol*. 2011;11(10):702–711. doi:10.1038/nri3064
46. Du R, Lu KV, Petritsch C, et al. HIF1alpha induces the recruitment of bone marrow-derived vascular modulatory cells to regulate tumor angiogenesis and invasion. *Cancer Cell*. 2008;13(3):206–220. doi:10.1016/j.ccr.2008.01.034
47. Zhou X, Yan T, Huang C, et al. Melanoma cell-secreted exosomal miR-155-5p induce proangiogenic switch of cancer-associated fibroblasts via SOCS1/JAK2/STAT3 signaling pathway. *J Exp Clin Cancer Res*. 2018;37(1):242. doi:10.1186/s13046-018-0911-3
48. De Palma M, Biziato D, Petrova TV. Microenvironmental regulation of tumour angiogenesis. *Nat Rev Cancer*. 2017;17(8):457–474. doi:10.1038/nrc.2017.51
49. Kisker O, Becker CM, Prox D, et al. Continuous administration of endostatin by intraperitoneally implanted osmotic pump improves the efficacy and potency of therapy in a mouse xenograft tumor model. *Cancer Res*. 2001;61(20):7669–7674.
50. Rahbari NN, Kedrin D, Incio J, et al. Anti-VEGF therapy induces ECM remodeling and mechanical barriers to therapy in colorectal cancer liver metastases. *Sci Transl Med*. 2016;8(360):360ra135. doi:10.1126/scitranslmed.aaf5219
51. Chandra A, Rick J, Yagnik G, Aghi MK. Autophagy as a mechanism for anti-angiogenic therapy resistance. *Semin Cancer Biol*. 2020;66:75–88. doi:10.1016/j.semcancer.2019.08.031